

# A new approach for studying vulnerability to Groundwater pollution using DRASTIC and AHP in the Biyeme Upper Stream Watershed, Yaoundé, Cameroon

François Ntep<sup>1,2\*</sup>, Jean Ghislain Tabue Youmbi<sup>1,2</sup>, Gabriel Alain Assoa Angoa<sup>2</sup>

<sup>1</sup> National Advanced School of Mines and Petroleum Industries, University of Maroua, P.O. Box 08 Kaele, Cameroon

<sup>2</sup> Department of Mining Petroleum Gas and Water Resources Exploration, University of Maroua, P.O. Box 08 Kaele, Cameroon

Received on 3 February 2025, Accepted on 18 January 2026

## Abstract

This research work presents the results of an assessment of the vulnerability of groundwater to surface pollution in the Biyeme Upper Stream Watershed (BUW). A method based on a geographic information system and the DRASTIC and AHP models was used to study this vulnerability. Located in the south-west of the city, the study area covers the part of Yaoundé where the population suffers from an inadequate supply of drinking water and where agriculture and/or livestock farming are the main means of subsistence. This research approach is based on continuous monitoring of average monthly data from 52 wells and 05 springs over 05 years, from 2015 to 2020. Assess the degree of vulnerability of groundwater to pollution in different areas of the catchment using each of the different methods and then compare them. In addition, a hierarchical analytical process was used to determine the assessment coefficients for each parameter. The main results show that the best outcome was achieved with DRASTIC-AHP. Regardless of the method used, vulnerability is highest in the upstream part of the basin; groundwater catchments in these areas must therefore be protected from contamination before they are sited.

© 2026 Jordan Journal of Earth and Environmental Sciences. All rights reserved

**Keywords:** Groundwater Vulnerability; DRASTIC and DRASTIC-AHP models; Biyéme Upper Stream Watershed; Yaoundé, Cameroon.

## 1. Introduction

Water is a finite resource under pressure from pollution, inadequate sanitation, increased frequency of groundwater droughts, overexploitation of groundwater at unsustainable rates, inadequate water infrastructure, increased food demand from a growing population, increased water consumption, and irrigation (Ghazavi and Ebrahimi, 2015; Hazaymeh and Lange, 2024). Agricultural and residential activities have made groundwater in the BUW vulnerable to pollution. Previous groundwater vulnerability assessment studies have shown that urban areas are increasingly vulnerable to groundwater contamination (Singh et al., 2015; Ghazavi and Ebrahimi, 2015; Hazaymeh and Lange, 2024). For several decades, the world's population has been growing rapidly, and Africa accounts for about 17.4% of that population. This growth systematically leads to increased consumption of renewable and non-renewable natural resources. To manage these resources effectively, we need to ensure that they are of good quality (Singh et al., 2015; Ghazavi and Ebrahimi, 2015; Hazaymeh and Lange, 2024). To do this, we need to understand and study the parameters that control groundwater vulnerability and identify areas likely to be contaminated. This study aims to produce groundwater vulnerability maps for the BUW. Groundwater uses in urban areas include not only abstraction by public services, but also private self-supply for residential, commercial, industrial and agricultural purposes (Alam et al., 2012). Urban self-

supply of water and the direct use of local wells by low-income households are often vital to a large proportion of a city's inhabitants (Kumar et al., 2015; La Vigna, 2022). A number of approaches have been developed to assess the vulnerability of groundwater. Three primary methods exist by which groundwater vulnerability is commonly assessed: (1) a subjective overlay and index method based on the rating of individual hydrogeological factors (Alam et al., 2012); (2) process based mathematical models that are data intensive (Neshat et al., 2014a) (3) statistical models that describe the contamination potential for a specified geographical region using the available data in the regions of interest (Alam et al., 2012).

## 2. Materials and methods

### 2.1. Study area

The BUW is located between 03°48'00" and 03°51'58" North latitude and between 11°27'36" and 11°30'00" East longitude, covering an area of 14.00 ha. It is part of the Mfoundi division (Fig.1). The hydrographic network constitutes a set of perennial rivers. The geological substratum is composed of a set of fractured Pan-African geotectonic units, constituting aquiferous reservoirs exploitable through wells and boreholes (Bissaya et al., 2018). Yaoundé is characterized by strongly accented relief, with a mean altitude of 730 m. Soils are red and ferrallitic in the majority.

\* Corresponding author e-mail: francoisntep10@gmail.com

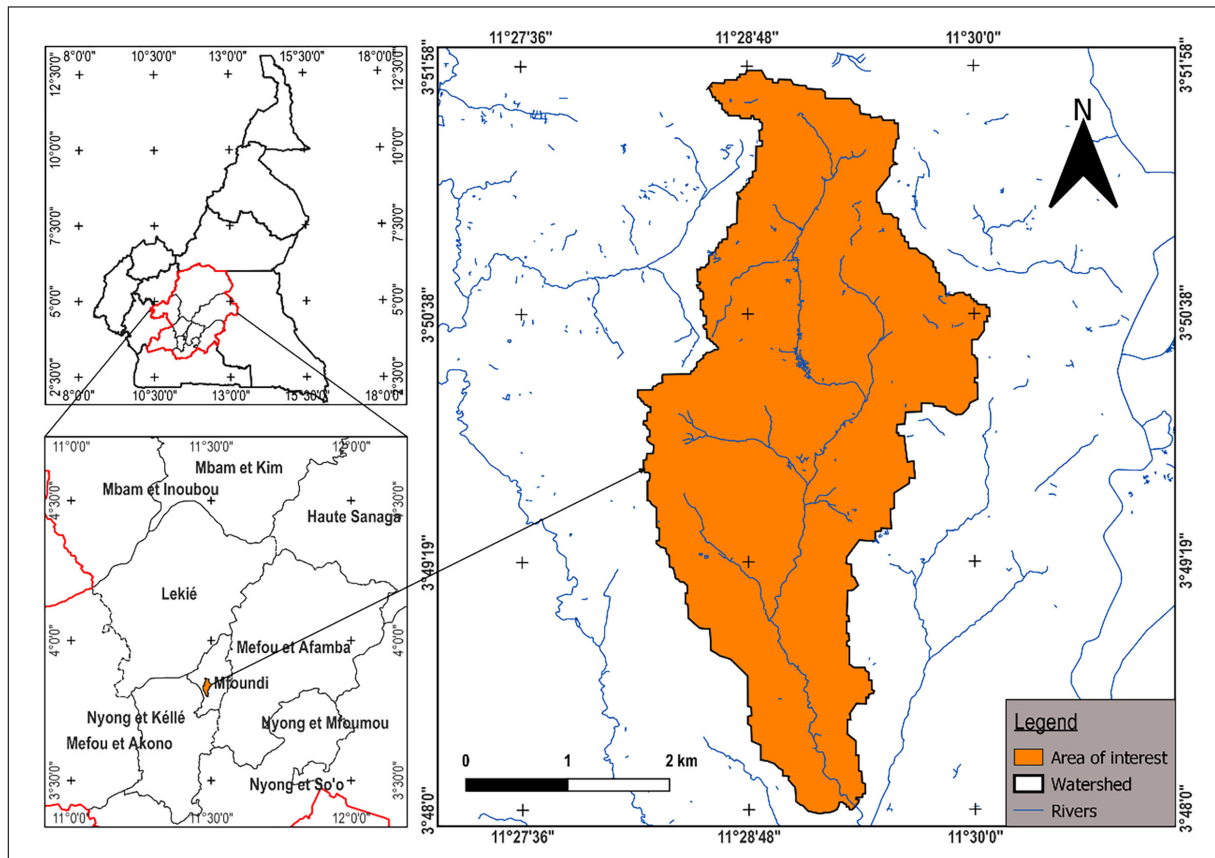


Figure 1. Geographical location of the Biyeme Upstream Watershed

The average inter-annual rainfall for the period from 1991 to 2021 is about 1727.00 mm. Potential Evapo-Transpiration (PET) has been calculated, using the Thornthwaite (1948) in (Fouépé et al., 2011; Ntep et al., 2021), and the average inter-annual PET is 964.00 mm. Figure 2 shows the variations in monthly rainfall in Yaoundé town from January to December, based on meteorological data recorded at the Yaoundé Air Force Station (Fouépé et al., 2011; Ntep et al., 2021). Heavy rainfall is drained by a set of perennial rivers, causing inundations of the valley bottom. The climate is equatorial, with two rainy seasons.

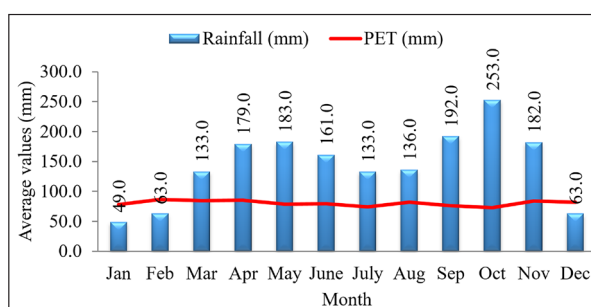


Figure 2. Monthly average rainfall and PET in Yaoundé city

The geology comprises crystalline basement rocks such as paragneiss, migmatitic gneiss, and schists of Proterozoic age, metamorphosed during the Pan-African orogeny at the northern margin of the Congo Craton (Bissaya et al., 2018). These medium- to high-grade metasediments are deeply weathered to form a lateritic soil profile up to 20 m thick (Fouépé et al., 2011; Kringel et al., 2016; Ntep et al., 2021). The bedrock is covered by alluvial hydromorphic clay and sand

in the valleys and ferralsols on the hillsides (Bissaya et al., 2018). The hydrogeological setting consists of an unconfined porous aquifer overlying a fractured gneiss aquifer of much lower productivity. The seasonal dynamics of unconfined groundwater flow are described by Ntep et al. (2021), who reported average groundwater level fluctuations of 0.49 m in valleys, 0.65 m on slopes, and 1.3 m on plateaus between the rainy and dry seasons. The groundwater surface generally follows the relief well. Kringel et al. (2016) charted the rapid expansion of the urban area. The population is expected to approach 2.5 million inhabitants at a growth rate of 5.7%. The relief in Yaoundé is undulating terrain with differences between 20 and 40 m at an average altitude of 730 m and seven prominent “inselbergs” with steep slopes (Fig.3).

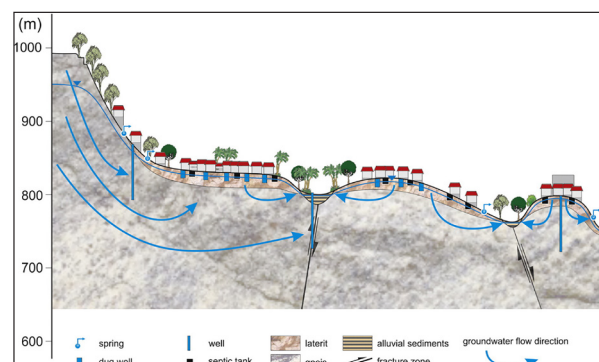


Figure 3. Sketch of the hydrogeological arrangement of terrain, aquifers, drainage network of Yaoundé in relation to urban settlement and decentralized installations of water supply and discharge; groundwater surface and flowlines only approximate - not to scale (Kringel et al., 2016).

2.2. Research methods and data collection

2.2.1. AHP method

The Multi-Criteria Decision Analysis (MCDA) is a process that integrates and transforms the judgment of a decision-maker and geographical data into useful and appropriate information for environmental decision-making (Focazio, 2002; Costa et al., 2019; Kargaranbafghi et al., 2020). It provides decision options, from the most preferred to the least preferred, using many techniques, such as the Analytic Hierarchy Process (AHP) and the set-theoretic approach (Velasquez and Hester, 2013; Gangadharan et al., 2016; Kargaranbafghi et al., 2020). To achieve this, Saaty (2001) developed the AHP. The AHP is an efficient tool for multiple decision-making, helping the decision-maker set priorities and make the best decision. The principle of this analysis is to compare the elements of each criterion 2 by 2 using a comparison scale. The aim here is to calculate new scores that will then be assigned to each criterion. Several combinations have been made DRASTIC-AHP.

In the DRASTIC-AHP method, the original DRASTIC scores are taken into account, and the weights of detailed parameters were established by ranking their importance and appropriateness based on their contribution to groundwater vulnerability assessment. Once the hierarchy has been established, multiple pairwise comparisons based on the standardized comparison scale of nine levels were estimated for all seven parameters. To achieve the desired results, there is a procedure to follow in Figure 4 and Table 1.

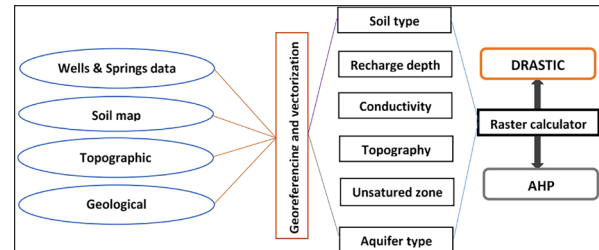


Figure 4. Flowchart of methodology for groundwater pollution vulnerability analysis (Oroji, 2018) modified.

Table 1. Comparison scale

Numeric scale or intensity	Verbal scale or definition	Comment
1	Equal importance of two elements Equally important	Both elements compete in the same way toward the goal
3	One element is a little more important than the other Slightly more important	Experience and personal judgment slightly favor one element over the other.
5	One element is more important than the other Strongly important	Experience and personal judgment really favor one element over the other
7	One element is much more important than the other Significantly more important	One element is largely dominant, and this dominance is demonstrated in practice.
9	One element is absolutely more important than the other Absolutely more important	The dominance of one element over another is demonstrated and absolute
2,4,6	Intermediate value between two judgments	Used to refine one's judgment
Reciprocity	If element i is assigned one of the previous numbers when compared to element j, then j will have the opposite value when compared to i	

2.2.1.1 Binary comparisons

Compare the relative importance of all the elements belonging to the same level of the hierarchy, taken two by two, in relation to the element of the level immediately above;

- For each comparison, choose the most important criterion and express your judgment as to its importance.
- The measure for determining relative importance could be expressed on a scale of 1 to 9.

Table 2 gives the scale values for comparing ratings when assessing the importance of two elements.

Table 2. Scale values for comparing the rating given when assessing the importance of two elements (Arauzo, 2017).

Expressing one criterion in relation to another	Rating
Same importance	1.00
Moderately important	3.00
Highly important	5.00
Very important	7.00
Extremely important	9.00
Moderately less important	0.33
Strongly less important	0.20
Less important	0.14
Extremely less important	0.11

2.2.1.2 Comparison judgment matrix

The criteria comparison given in Table 1 is transformed into a judgment matrix by transcribing the evaluation values into the corresponding columns (Table 3). The value “a” is entered in cell “i” column and “j” row of a criterion considered important. Then the value ratio of “1/a” is entered in the cell considered less important in the comparison.

Table 3. Judgment matrix for depth parameter

Depth (m)	1.50-4.50	4.50-9.00	9.00-15.00	15.00-23.00
1.50 - 4.50	1.00	3.00	5.00	5.00
4.50 - 9.00	0.33	1.00	3.00	5.00
9.00 - 15.00	0.20	0.33	1.00	3.00
15.00 - 23.00	0.20	0.20	0.33	1.00
Total	1.73	4.53	9.33	14.00

a = value found in the intersection of cell i column and j row, and noted (a<sub>ij</sub>).

C<sub>1</sub>, C<sub>2</sub> to C<sub>n</sub> = comparison criterion set in row “i” and column “j” corresponding to the evaluation comparison value C<sub>i</sub> and C<sub>j</sub>.

$$A = [a_{ij}] = \begin{bmatrix} 1 & a_{12} & \dots & a_{1n} \\ \frac{1}{a_{12}} & 1 & \dots & a_{2n} \\ \vdots & \vdots & \ddots & \vdots \\ \frac{1}{a_{1n}} & \frac{1}{a_{2n}} & \dots & 1 \end{bmatrix} \tag{1}$$

The matrix in the previous table is as follows:

$$A = \begin{bmatrix} 1.00 & 3.00 & 5.00 & 5.00 \\ 0.33 & 1.00 & 3.00 & 5.00 \\ 0.20 & 0.33 & 1.00 & 3.00 \\ 0.20 & 0.20 & 0.33 & 1.00 \end{bmatrix} \tag{2}$$

**Calculating the vectors of the priority**

This outcome involves calculating the eigen vectors of the matrix obtained from the previous evaluations. Tables 4 and 5 give the respective division of each element of the matrix by the total of its column and the calculation of the average of the elements in each row of the previous matrix.

**Table 4.** Division of each element of the matrix by the total of its column

Depth (m)	1.50-4.50	4.50-9.00	9.00-15.00	15.00-23.00
1.50 - 4.50	0.58	0.66	0.54	0.36
4.50 - 9.00	0.19	0.22	0.32	0.36
9.00 - 15.00	0.12	0.10	0.11	0.21
15.00 - 23.00	0.12	0.04	0.04	0.10

**Table 5.** Calculation of the average of the elements in each row of the previous matrix

Depth (m)	1.50-4.50	4.50-9.00	9.00-15.00	15.00-23.00	Priority
1.50-4.50	1.00	3.00	5.00	5.00	2.32
4.5-9.00	0.33	1.00	3.00	5.00	1.20
9.00-15.00	0.53	0.27	0.13	0.10	0.53
15.00-23.00	0.20	0.20	0.33	1.00	0.27

**Calculating of the intrinsic value λmax**

The matrix A is multiplied by the elements of the priority vector (x), x is the eigenvalue of the priority vector (n), and the average of the values found is calculated. The result is

called the λmax value. Let a<sub>ij</sub> = the judgment matrix of the value of the element (i) in the ith row and the element (j) jth column. The normalised value a<sub>ij</sub> is equal to

$$a_{ij} = W_i/W_j, \text{ and } a_{ji} = W_j/W_i = 1/a_{ij}, \tag{3}$$

(3) reciprocal

W<sub>i</sub> = contribution to the selection of the best choice and to each of the criteria

W<sub>j</sub> = contribution of the specific criteria to the main objective.

Jhariya et al. (2019), then Saaty (2001), suggested that the largest eigen value

$$[(\lambda_{max} = a)]_{ji} = W_j/W_i = 1/a_{ij} \tag{4}$$

The results of the Judgment matrix for the depth parameter and the division of the elements of the sum vector weighted by the priority corresponding to each criterion are shown in Table 6.

**Table 6.** Weighted sum corresponding to each criterion's priority

Depth (m)	1.50-4.50	4.50-9.00	9.00-15.00	15.00-23.00	Priority
1.50-4.50	0.58	0.66	0.54	0.36	0.53
4.50-9.00	0.19	0.22	0.32	0.36	0.27
9.00-15.00	0.12	0.10	0.11	0.21	0.13
15.00-23.00	0.12	0.04	0.04	0.10	0.10

This is how we calculate the average value of λmax

$$[(4.36 + 4.28 + 4.12 + 4.06)]/4 = 4.20 \tag{5}$$

**Random Index [RI]**

Jhariya et al. (2019) then Saaty (2001), developed a scale in which random indexes [RI] were established by making random judgment across a large number of replications. This [RI] number represents the average of the indices calculated across replications for different square matrix sizes (N). The reading of the [RI] value is indicated by a random index in Table 7. N=5 RI= 1.12

**Table 7.** Random index

N	1	2	3	4	5	6	7	8	9	10	11	12	13	14	15
RI	0.00	0.00	0.58	0.90	1.12	1.24	1.32	1.41	1.45	1.49	1.51	1.48	1.56	1.57	1.59

**Calculating the Coherence Index (CI)**

The various steps involved in calculating the new ribs result in redundant comparisons, aimed at improving the quality of the result. The CI is a tool that provides information about the validity of the results.

$$IC = (\lambda_{max} - N)/(N - 1)CI = (\lambda_{max} - N)/(N - 1) \tag{6}$$

with N=5, CI= 0.07

**Calculating the Coherence Ratio (CR)**

The coherence ratio is the ratio of the coherence index calculated on the matrix corresponding to the decision-maker's judgments and the random index of a matrix of the same dimension. If CR ≤ 10% or 0.10, the matrix is considered to be sufficiently coherent. If this value exceeds 10%, the assessments may need to be revised.

$$CR = IC/IARC = CI/RI \tag{7}$$

with CI= 0.07 and RI=0.9, so CR<10%,

The degree of consistency of the comparison is acceptable. Once the new coastlines have been validated, we apply the same principle as in the DRASTIC method to calculate the vulnerability indices. This gives:

$$S = \sum_{i=1}^N W_i X_i \tag{8}$$

with S as the index, W<sub>i</sub> as the parameter weight, and X<sub>i</sub> as the criterion rating.

The higher the scores, the higher the values of the vulnerability indices and the more vulnerable the areas.

**2.2.1.3. Mapping of vulnerability zones using the DRASTIC-AHP method**

The new vulnerability indices have been calculated using the AHP method, as illustrated above. The DRASTIC-AHP and AHP-AHP vulnerability maps are thus obtained using Table 8.

**Table 8.** Classification of vulnerabilities according to the DRASTIC-AHP method (Magha et al., 2021)

Value	Degree of Vulnerability
0.10	Very Low
0.20	Low
0.30	
0.40	Medium
0.50	
0.60	
0.70	High
0.80	
0.90	Very high

**2.2.2. DRASTIC method**

This method takes into account the litho-petrophysical parameters of the layers overlying the water table (Aller et al., 1987; Babiker et al., 2005; Sarah, 2016). Each parameter is assigned a weight, and each reference value or range of values is assigned a slope; the weighted slope is obtained by simply multiplying the two. The result will be a cartographic rendering produced in ARCGIS software from a grid designed in EXCEL. The vulnerability index will be calculated according to the following equation (9), and Table 8 provides the attribution of notes for the DRASTIC model indicators (Chi et al., 2017).

$$I = DvDw + RvRw + AvAw + SvSw + TvTw + IvIw + CvCw \tag{9}$$

Where “v” is the rib and “w” the weight.

**Table 9.** Attribution of notes for DRASTIC model indicator (Aller et al., 1987; Oroji, B., 2018).

Range	Rating		Range	Rating		Range	Rating			
Confining Layer	1	Zone vadose	0.0-1.5	10	Depth to water (m)	0.04-4.1	1	Conductivity (m)		
Silt/Clay	3		1.5-4.5	9		4.1-12.3	2			
Shale	3		4.5-9.0	7		12.3-28.7	4			
Limestone	3		9.0-15.0	5		28.7-41	6			
Sandstone	6		15-22	3		41-82	8			
Bedded Limestone. Sandstone	6		22-30	2		>82	10			
Sand and Gravel W. Silt	6		>30.4	1		10	10			
Sand and Gravel	8	Aquifer media	Thin or Absent	10	Soil media	2-6	9	Topography (m)		
Basalt	9		Gravel	10		6-12	5			
Massive Shale	2		Sand	9		12-18	3			
Metamorphic/Igneous	3		Peat	8		>18	1			
Weathered Metamorphic Igneous	4		Shrinking Clay	7		0-50	1	Recharge (mm)		
Glacial Till	5		Sandy Loam	6						
Bedded Sandstone. Limestone	6		Loam	5					50-100	3
Massive Sandstone	6		Silty Loam	4						
Massive Limestone	8		Clay Loam	3		100-175	6			
Sand and Gravel	8		Muck	2		175-225	8			
Basalt	9	No shrinking Clay	1	>225	9					
Karst Limestone	10									

**2.3 Maps validation**

For several authors, Lerner (2004), Shrestha et al. (2016), Aydi (2018), and Khosravi et al. (2018), the validation of the maps is based on chemical analyses of the various water samples taken. A comparison is made between the distribution of water quality and the spatial distribution of water vulnerability derived from the vulnerability maps. Areas of low vulnerability are associated with low-quality water, while areas of high vulnerability are associated with polluted water. Once the necessary data were collected to prepare the vulnerability map, the DRASTIC vulnerability index was computed by linearly combining all seven model parameters. Data analysis and model implementation included assigning sensitivity ratings to mapped attributes and combining or overlaying individual characteristic maps to create the final cumulative vulnerability map using GIS (Shrestha et al., 2016; Khosravi et al., 2018).

**2.4. Comparison of the maps obtained**

According to Aller et al. (1987) and Babiker et al. (2005), comparing assessment methods comes down to determining whether the methods are correlated two by two and which method offers the greatest margin of safety. Surface analysis is used to determine the difference between the vulnerability maps produced by the different methods. This analysis assumes that the index values are identical from one map to another and that the maps are consistent.

**3. Results and Discussion**

**3.1. Results**

**3.1.1. DRASTIC results**

DRASTIC parameters were collected, analyzed, and overlapped to generate a groundwater vulnerability map as follows:

3.1.1.1. Depth (D)

The depth of groundwater is the vertical distance between the ground surface and the water level. This parameter determines the time required for water-soluble pollutants to penetrate from the ground to the aquifer. Thus, near-surface aquifers are likely to become contaminated faster than deeper aquifers (Chandoul et al., 2008). The th was directly measured by subtracting the water surface level from the top aquifer level. The depths vary between 5.0 m and 9.0 m. Depths of 7.0 m are the most represented, while depths of 5.0 m are the least, with less vulnerability observed regarding depth to water layer". The different ratings assigned to each interval are given in Table 9, and the map in Figure 5 shows the depths in the BUW during the monitoring period. From Figure 5, it can be observed that shallow aquifers occupy a very small percentage of the basin area and are confined to the upper part of the basin.

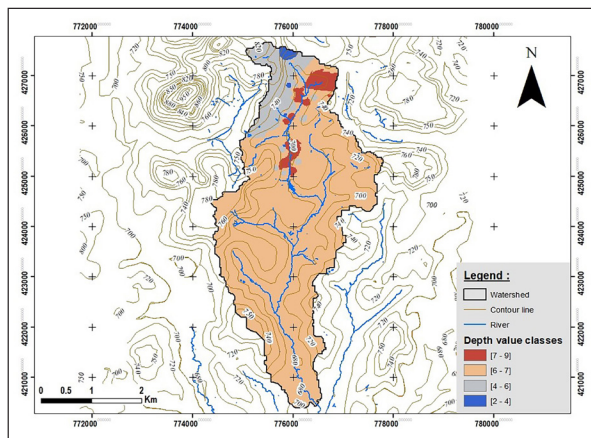


Figure 5. Mapping of depths to water table in the BUW.

3.1.1.2. Recharge (R)

According to Mansaray et al. (2015) then Nkembe & Defo (2022), three types of recharging mechanisms are generally defined. The variability of recharge estimation methods poses a significant challenge in choosing the most suitable one. Mansaray et al. (2015) then Nkembe & Defo (2022), demonstrated that the judicious choice of these methods should relate to a technique on a spatiotemporal scale, a range of values representative of the geological and hydrogeological conditions in the field, and the validity of the methods based on various techniques. The piezometric level fluctuation method enables quantification of effective infiltration in free water tables. It enables establishing a link between precipitation and variations in the piezometric level of the water table. The Water Table Fluctuation (WTF) method requires knowledge of the storage coefficient and the piezometric amplitude of the water table over time, which are deduced from the topographic level of each well. Recharge is estimated by the WTF method. Figure 6 shows the representation of recharge in the basin during the monitoring period. Over almost the entire study area, recharge ranged from 0.005 mm to 0.20 mm per day. Table 9 shows the ratings assigned for recharge using the DRASTIC method. Layers of precipitation, soil, and slope percentage were overlaid. According to DRASTIC ratings, the net groundwater recharge layer indicates medium to

high vulnerability (Sarah, 2016). From Figure 6, it can be concluded that in this basin, the recharge values decrease from the upstream to the downstream of the main draining river.

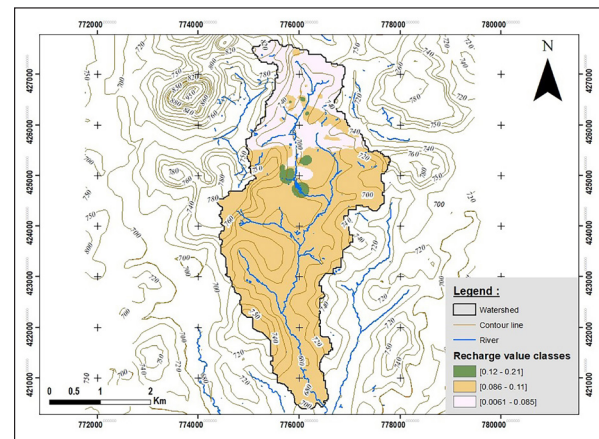


Figure 6. Mapping of the recharge variation in the BUW.

3.1.1.3. Aquifer media

The aquifer media reflects the characteristics of the constituents of the aquifer vadose zone that affect water flow within the aquifer and control pollutant attenuation processes (Chandoul et al., 2008). The BUW aquifer is essentially composed of granular elements derived from the alteration of the gneiss. The materials are, therefore, for the most part, a heterogeneous mixture of fine to coarse sand in equal proportions with the products of altered metamorphites. Figure 7 shows the distribution of materials in the aquifer, and Table 9 shows the corresponding rating.

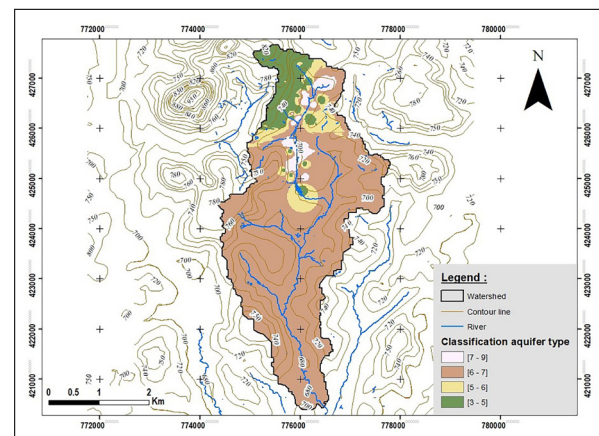


Figure 7. Mapping of the aquifer materials in the BUW.

3.1.1.3. Aquifer media

The aquifer media reflects the characteristics of the constituents of the aquifer vadose zone that affect water flow within the aquifer and control pollutant attenuation processes (Chandoul et al., 2008). The BUW aquifer is essentially composed of granular elements derived from the alteration of the gneiss. The materials are, therefore, for the most part, a heterogeneous mixture of fine to coarse sand in equal proportions with the products of altered metamorphites. Figure 7 shows the distribution of materials in the aquifer, and Table 9 shows the corresponding rating.

3.1.1.4. Soil type

Soil has a significant effect on the amount of recharge; therefore, it affects the ability of a pollutant to move vertically in the vadose zone. According to Aller et al. (1987) and Sarah (2016), fine-grained materials such as clay and silt reduce soil permeability and, thus, limit the movement of contaminants. The various soil formations have been estimated from Figure 8 and highlighted using the classification provided in Table 9 of the DRASTIC rating.

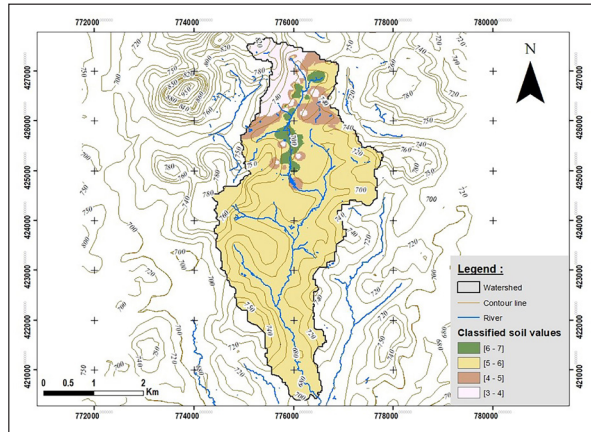


Figure 8. Mapping of the soil type in the BUW.

3.1.1.5. Topography

Although the BUW belongs to highly geomorphological units at altitudes of over 700 m, almost all the slopes are between 5 and 6% (Fig.9). Slopes in excess of 6% cover the North-West of the basin. There are only a few areas with slopes exceeding 10%. The land slope is a critical factor that determines the amount of surface runoff. As a result, low-slope areas tend to retain water for a longer period, leading to greater infiltration and, thus, a higher pollution potential (Moges and Dinka, 2012).

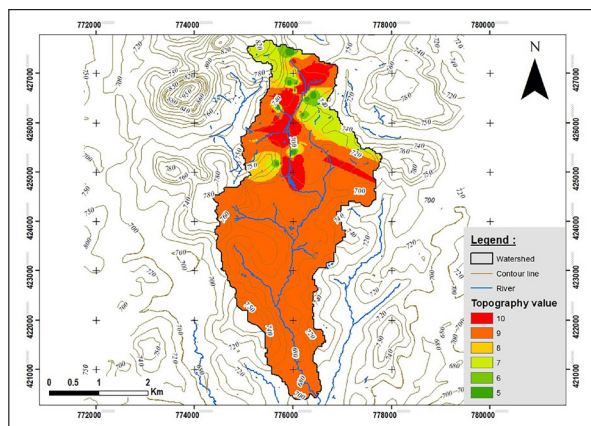


Figure 9. Mapping of the topography classes in the BUW.

3.1.1.6. Impact of the vadose zone

The vadose zone is composed of silty and clayey sands in almost equal proportions. It is made up of sands and clays in the South-West, East, Center to North, and North-West of the study area, and sands and silts from the center to the South-East and North-West of the basin. The sand-silt-clay combination is scattered in the northern part of the study area. According to Aller et al. (1987) and Sarah (2016), fine-grained materials such as clay and silt reduce soil permeability and, thus, limit the movement of contaminants.

Figure 10 shows a cartographic representation of the vadose zone classes in the basin.

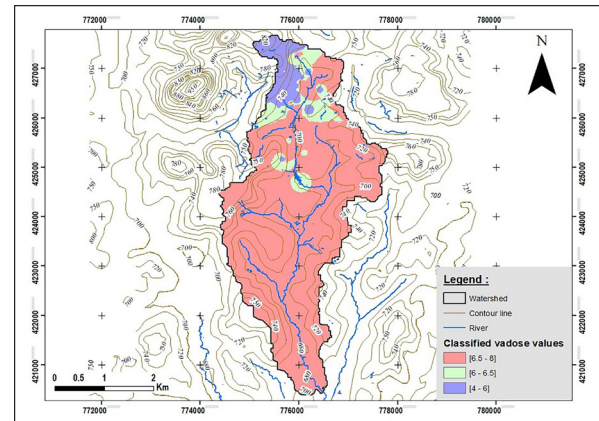


Figure 10. Mapping of the vadose zone classes in the BUW.

3.1.1.7. Hydraulic conductivity

This parameter plays an essential role in the rate of dispersal and migration of pollution (Chandoul et al., 2008). Higher hydraulic conductivity indicates greater infiltration and movement of water and contaminants into the aquifer, increasing the potential for pollution. The map in Figure 11 shows the conductivity classes recorded in the BUW.

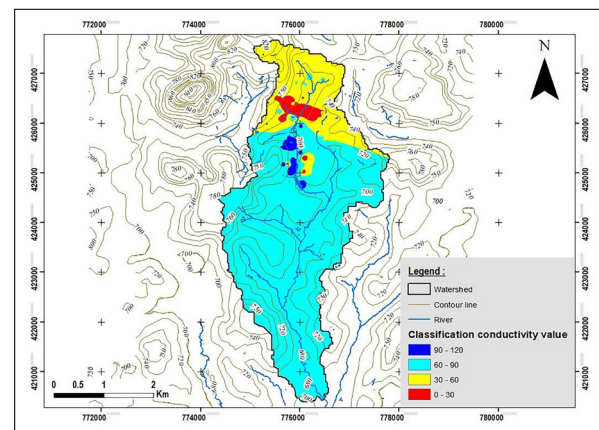


Figure 11. Mapping of the conductivity classes in the BUW.

3.1.1.8. Mapping of DRASTIC vulnerability areas

Calculation of the DRASTIC vulnerability indices gave values ranging from 70 to 159, with percentages of 23.5 and 66.99, respectively. These indices, calculated as a percentage, show the existence of three classes of vulnerability: low, medium, and high (Table 10). The high vulnerability class covers approximately 88% of the surface area of the BUW (Fig.12). The DRASTIC parameter weights are given in Table 10.

Table 10. Evaluation criteria of degree of vulnerability models.

Vulnerability	Method					
	DRASTIC		AHP-AHP		DRASTIC-AHP	
	Area		Area		Area	
	ha	(%)	ha	(%)	ha	(%)
Low	0.3	02	1.8	13	0.7	05
Medium	1.4	10	11.9	85	11.2	80
High	12.3	88	0.3	02	2.1	15

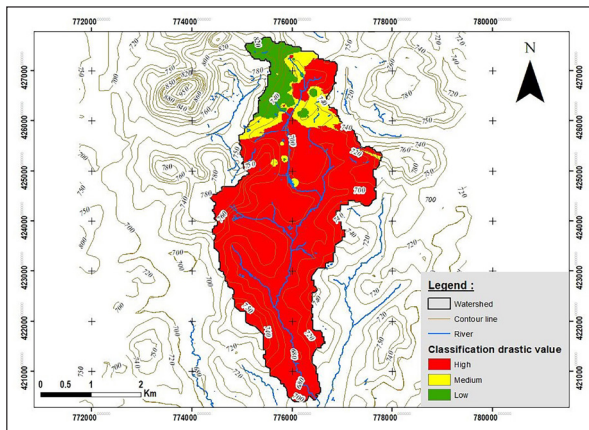


**Figure 12.** The DRASTIC model vulnerabilities classes map in the BUW.

### 3.1.2. AHP-AHP result

Figure 13 shows the vulnerability of the study area using the AHP-AHP method. As with previous methods, there are three classes of vulnerability. The medium vulnerability class covers approximately 70% of the basin's total surface area. The low- and high-vulnerability classes cover the rest of the area.

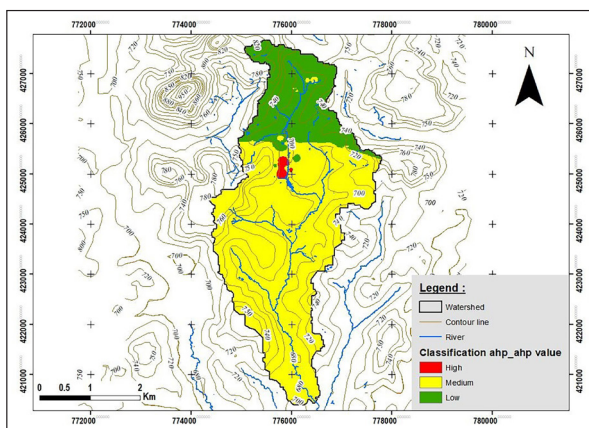


**Figure 13.** The AHP-AHP model vulnerabilities classes map in the BUW.

### 3.1.3. DRASTIC-AHP result

Figure 14 shows the vulnerability situation obtained using the DRASTIC-AHP method. It shows three classes of vulnerability, with the medium class predominating. The high and low classes occupy about 20% of the basin's surface area. According to this index, this aquifer has low vulnerability potential.

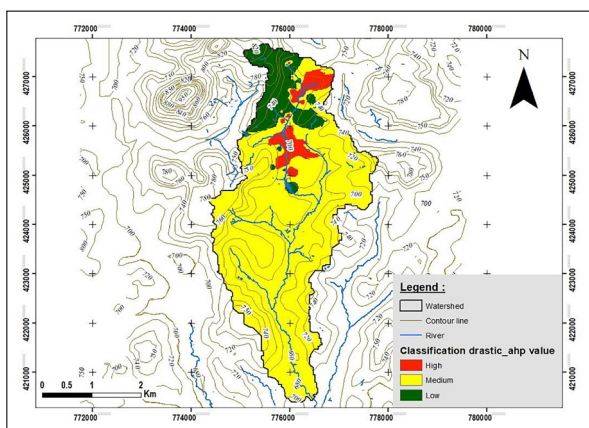


**Figure 14.** The DRASTIC-AHP method vulnerability classes map in the BUW.

## 3.2. Discussion

According to Mansaray et al. (2015), Sarah (2016), Nkembe & Defo (2022), and the rest of the city of Yaoundé, the BUW is essentially alluvial, made up of sand, silt, and clay. The sand particle size varies from 0.05 mm to 2.0 mm, the silt from 0.002 mm to 0.05 mm, and the clay fraction consists of a mixture of clay and sand. The relative proportions of sand, silt, and clay that make up this soil. Many soil properties are influenced by texture, including drainage, water holding capacity, aeration, susceptibility to erosion, organic matter content, cation exchange capacity, pH buffering capacity and soil thickness (Mansaray et al., 2015; Nkembe & Defo, 2022). According to the results, the category 0.04 to 4.1 m/day as hydraulic conductivity values, has the largest area. Therefore, the amount of hydraulic conductivity is low, and since the potential for vulnerability is directly related to this parameter, the amount of vulnerability is low. The geological structure of the sand of the aquifer media contains most of the region, which is graded eighth in the aquifer media ranking. A large percentage of the study area is composed of sandy loam texture, which according to the soil texture rankings, is ranked sixth and has a moderate vulnerability. The quantity of water that a given soil can store, mainly influenced by soil texture and organic matter content. In general, soils with particles of silt and clay have a greater capacity to retain water. Similarly, soils richer in organic matter have a greater water retention capacity (Moges and Dinka, 2012). Which leads to groundwater contamination in this basin due to poor drainage of runoff water (Moges and Dinka, 2012). The table 6 compares the different methods. Whatever the method, only three classes of vulnerability were detected. In the DRASTIC method, the vulnerability class dominates over the other two, whereas the average vulnerability class predominates in the AHP-AHP and DRASTIC-AHP methods, in almost equal proportions in the basin and for this study period. It can therefore be seen that the AHP-AHP and DRASTIC-AHP methods minimise the vulnerability of subsurface groundwater in this Biyeme upper stream basin compared with the DRASTIC derived method and are therefore the most suitable for decision-making in the context of groundwater protection in general and in this basin in particular. Some parameters were obtained indirectly and by interpolation, in particular recharge, conductivity and lithology, which may explain the discrepancies in the final results. According to the method used, the predominant classes of vulnerability are medium and high. The areas of very low vulnerability are located on the higher ground, where the soil profile is well developed with sufficient clay, low conductivity and low recharge. It should be noted that these maps are decision-making aids for the efficient management of groundwater resources. They can be used to establish resource protection areas.

## 4. Conclusions

Groundwater vulnerability assessments of the entire basin are found to be realistic and suitable for the area. However, despite its success in some case studies, the DRASTIC method has some disadvantages. The influence of regional characteristics (geology, hydrology, hydrogeology, land use etc.) is not accounted for in the method, so the same weights and rating values are used everywhere. This research paper also provides an overview of the vulnerability

of drinking water supply systems, which is quantified using a quantitative vulnerability assessment index. Groundwater resources, which account for 96% of the world's freshwater, are highly valuable because they are potable and require minimal treatment. However, this resource remains under-exploited in poor and developing countries. Given the complaints of people living in urban areas about untimely water cuts and water rationing, the management of water resources in these countries needs to be seriously questioned. To this end, strategies and policies have been put in place to address this problem, notably through the PAEPYS (Projet d'Alimentation en Eau Potable de la ville de Yaoundé à partir de la Sanaga). This project will eventually supply 315.000 m<sup>3</sup> of water per day to the urban and peri-urban populations of Yaounde city. Unfortunately, this project relies on surface water resources, yet underground resources also exist and could serve as a potential source of supply for the populations in situations where the CAMWATER water distribution network is absent or non-operational. This could help communities to become self-sufficient in terms of drinking water supply on a sustainable and, above all, permanent basis. For this reason, it should first be protected. Although it lies deep underground, this water is just as vulnerable as surface water. Potential sources of pollution have been identified. Household waste and poorly regulated septic tanks are the main sources of groundwater vulnerability in the BUW. The concentration of populations in medium-slope areas could explain why the high-vulnerability classes in these waters are present in medium- to low-slope areas. This mapping enabled three classes of vulnerability to be assessed: low, medium and high, based on the natural parameters of the aquifer. The "very high" class is absent, whatever the method. The DRASTIC method might be considered a helpful approach for qualitatively evaluating vulnerability to different sources of pollution and assisting planners and decision-makers in preserving groundwater resources in the BUW. According to this evaluation, the DRASTIC-AHP method has higher accuracy than the other methods, with 88% accuracy. For this reason, it can be concluded that the modified-DRASTIC-AHP method gave more valid and accurate results than other methods for the alluvial aquifer vulnerability assessments. The groundwater vulnerability maps for the BUW area are ideal for future land-use planning studies. Detailed and frequent groundwater quality monitoring in highly vulnerable areas should be performed to monitor changing levels of pollutants. In addition, local administrators should conduct education programs and awareness-raising activities for the farmers. However, other quantitative, process-based models are recommended for precise outcomes.

#### Nomenclature

BUW = Biyeme Upper Stream Watershed;

NASMPI = National Advanced School of Mines and Petroleum Industries;

PET = Potential Evapo Transpiration;

AHP = Analytic Hierarchical Process;

WTF = Water Table Fluctuation

CAMWATER = Cameroon water utilities.

#### Acknowledgments

The author is really grateful to the reviewers and editors for their stimulating and constructive suggestions.

#### Conflict of interest statement

The author declares that he has no known competing financial interests or personal relationships that could have influenced the work reported in this paper.

#### References

- Alam, M., Rais, Aslam, S.M. (2012). Hydrochemical Investigation and Quality Assessment of Ground Water in Rural Areas of Delhi, India. *Environmental Earth Sciences*, 66, 97-110. <https://doi.org/10.1007/s12665-011-1210>.
- Aller, L., Bonnet, T., Lehr, J., Petty, R. and Hackett, G. (1987). DRASTIC: a standardized system for evaluating groundwater pollution potential using hydrogeological settings. Report No 600/287/035, EPA, Washington, USA. J. Environ Protection Agency.
- Arauzo, M. (2017). Vulnerability of groundwater resources to nitrate pollution: A simple and effective procedure for delimiting Nitrate Vulnerable Zones. *Sci Total Environ*; 575:799-812. doi:10.1016/j.scitotenv.2016.09.139.
- Aydi, A. (2018). Evaluation of groundwater vulnerability to pollution using a GIS-based multi-criteria decision analysis. *Groundw Sustain Dev*. 7:204-11. doi:10.1016/j.gsd.2018.06.003.
- Babiker, I.S., Mohamed, M.A.A., Hiyanna, T. and Kato, A. (2005). A GIS Based DRASTIC Model for Assessing Aquifer Vulnerability in Kakamigahara Heights, Gifu Prefecture, Central Japan. *Science of the Total Environment*, 345, 127-140. <http://dx.doi.org/10.1016/j.scitotenv.2004.11.005>.
- Bissaya, R., Ghogomu, R.T., Akissebini, S.M. (2018). Geomorphological approach in active tectonics for the cartography of landslide and rock fall hazards in the North-West part of the region of Yaounde-Cameroon. *The International Journal of Engineering and Science (IJES)*. Volume 7, 4 (2018) PP 73-96.
- Chandoul, E.R., Trabelsi, N., Bouaziz, S. and Ben Dhia H. (2008). "Spatial Analyst" pour le calcul et la cartographie de la vulnérabilité des eaux souterraines à la pollution selon la méthode DRASTIC. Application sur la nappe phréatique de Gabès Nord, La conférence Francophone ESRI, Versailles.
- Chi, Z., Yuntao, W., Li, Y. and Ding, W. (2017). Vulnerability Analysis of Urban Drainage Systems: Tree vs. Loop Networks Sustainability, 9, 397.
- Costa, C.W., Lorandi, R., Lollo, J.A., Santos, V.S. (2019). Potential for aquifer contamination of anthropogenic activity in the recharge area of the Guarani Aquifer System, southeast of Brazil. *Groundwater for Sustainable Development*. Vol. 8 p. 10–23. DOI 10.1016/j.gsd.2018.08.007.
- Focazio, M.J. (2002). Assessing groundwater vulnerability to contamination: providing scientifically defensible information for decision makers (Vol. 1224). US Dept. of the Interior, US Geological Survey.
- Fouébé, A., Ndam Ngoupayou, J.R., Riote, J., Takem, J.E., Mafany, G., Maréchal, J.C., Ekodeck, G.E. (2011). Estimation of groundwater recharge of shallow aquifer on humid environment in Yaounde, Cameroon using hybrid water-fluctuation and hydrochemistry methods. *Environ Earth Sci* 64: 107–118 doi 10.1007/s12665-010-0822-x.
- Gangadharan, R, Nila Rekha, P., Vinoth, S. (2016). Assessment of groundwater vulnerability mapping using AHP method in coastal watershed of shrimp farming area. *Arab J Geosci* 2:107
- Ghazavi, R. and Ebrahimi Z. (2015). Assessing groundwater vulnerability to contamination in an arid environment using DRASTIC and GOD models. *International Journal of Environmental Science and Technology*, (12), 2909–2918.

- <https://doi.org/10.1007/s13762-015-0813-2>.
- Hazaymeh and Lange (2024). A review on water quality aspects of urban rainwater harvesting in Jordan/ JJEES 15 (3): 199-207.
- Jhariya, D.C., Kumar, T., Pandey, H.K., Kumar, S., Kumar, D., Gautam, A., Baghel, V. and Kishore, N. (2019). Assessment of Groundwater Vulnerability to Pollution by Modified DRASTIC Model and Analytic Hierarchy Process. *Environmental Earth Sciences*, 78, 610. <https://doi.org/10.1007/s12665-019-8608-2>.
- Kargaranfahghi, F., Kheirandish Ravari, M., Rahimi Shahid, M. (2020). Seismic hazard analysis of Zarand city using AHP-GIS. *Italian Journal of Engineering Geology and Environment* 1: 5-16.
- Khosravi, K., Sartaj, M., Tasai, F., Singh, V., Kazakis, N., Melesse A. (2018). A comparison study of DRASTIC methods with various objective methods for groundwater vulnerability assessment. *Sci Total Environ.* 642 : 1032-49. doi:10.1016/j.scitotenv.2018.06.130.
- Kringel, R., Rechenburg, A., Kuitcha, D., Fouépé, A., Bellenberg, S., Kengne, I.M., Fomo MA. (2016). Mass balance of nitrogen and potassium in urban groundwater in Central Africa, Yaounde/Cameroon. *Science of the Total Environment* 547, 382–395 <http://dx.doi.org/10.1016/j.scitotenv.12.090>.
- Kumar, P., Bansod, B.K.S., Debnath, S.K., Thakur, P.K., Ghanshyam, C. (2015). Index-based groundwater vulnerability mapping models using hydrogeological settings: a critical evaluation *Environmental impact assessment review*, 2015 51 38.
- La Vigna F. (2022). Urban groundwater issues and resource management, and their roles in the resilience of cities *Hydrogeology Journal* <https://doi.org/10.1007/s10040-022-02517-1>.
- Lerner, D.N. (2004). "Urban groundwater pollution. International contributions to hydrogeology IAH" "Urban groundwater pollution", 24. A. A. Publ., 277 pp.
- Magha, A., Awah, M., Nono, G., Tamfuh, P., Wotchoko, P., Adoh, M. and Kabeyene, V. (2021). Assessment of Groundwater Quality for Domestic and Irrigation Purposes in Northern Bamenda (Cameroon). *Journal of Water Resource and Protection*, 13, 1-19. doi: 10.4236/jwarp.2021.131001.
- Mansaray, A., Gogra, A. and Massaquoi A. (2015). The Recharge Potential of Groundwater in the Mokonde Community in Southern Sierra Leone. *Natural Resources*, 6, 543-552. doi: 10.4236/nr.2015.611052.
- Moges, S.S. and Dinka, M.O. (2012). Assessment of groundwater vulnerability mapping methods for sustainable water resource management: An overview. *Journal of Water and Land Development* DOI: 10.24425/jwld.140389, No. 52 (I-III): 186–198.
- Neshat, A., Pradhan, B., Pirasteh S., Shafri, HZM (2014a). Estimating groundwater vulnerability to pollution using a modified DRASTIC model in the Kerman agricultural area, Iran. *Environ Earth Sci* 71(7):3119–3131.
- Ntep, F., Tabue Youmbi, J.G., Feumba, R., Ewodo Mboudou, G., Ngos III, S. (2021). Analyse piézométrique et suivi de la pollution des ressources en eau des aquifères de subsurface du Bassin Versant Amont de la Biyeme (BVAB) Yaoundé Cameroun. *Afrique SCIENCE*, 18, 6, 132 – 149 pp.
- Nkembe, S.E., Defo, C. (2022). Assessment of piezometric distribution and vulnerability of groundwater to pollution in a tropical environment: the case study of the aquifer of Santchou, Cameroon, Central Africa. *Sustainable Water Resources Management*, 8(2): 48. <https://doi.org/10.1007/s40899-022-00605-4>.
- Oroji, B. (2018). Groundwater vulnerability assessment using GIS-based DRASTIC and GOD in the Asadabad plain. *J. Mater. Environ. Sci.*, Volume 9, Issue 6, Page 1809-1816.
- Saaty, T. (2001). *Decision Making for Leaders: The Analytic Hierarchy Process for Decisions in a Complex World*. RWS Publications, Pittsburg.
- Sarah, W. (2016). "A Vulnerability Framework for Assessing the Risks to Water Supply Systems Under Climate Uncertainty in the Urban North eastern United States" Doctoral Dissertations. <https://doi.org/10.7275/7872988.0>.
- Shrestha, S., Kafle, R. and Pandey V. (2017). Evaluation of index-overlay methods for groundwater vulnerability and risk assessment in Kathmandu Valley, Nepal. *Sci Total Environ.* 575:1-12. doi: 10.1016/j.scitotenv.2016.09.141.
- Singh, P., Tiwari, A.K., Singh, P.K. (2015). Assessment of groundwater quality of Ranchi township area, Jharkhand, India by using water quality index method. *Int J Chem Tech Res* 7 (01): 73–79.
- Velasquez, M. and Hester, P.T. (2013). An analysis of multi-criteria decision-making methods. *International Journal of Operations Research*. Vol. 10(2) p. 56–66.